Environ. Sci. Technol. **2005**, *39,* 5262−5267

Electricity Generation from Artificial Wastewater Using an Upflow Microbial Fuel Cell

ZHEN HE,[†] SHELLEY D. MINTEER,[‡] AND LARGUS T. ANGENENT*,[†]

Environmental Engineering Science Program and Department of Chemical Engineering, Washington University in St. Louis, St. Louis, Missouri 63130, and Department of Chemistry, Saint Louis University, St. Louis, Missouri 63103

The upflow microbial fuel cell (UMFC) was developed to generate electricity while simultaneously treating wastewater. During a five-month period of feeding a sucrose solution as the electron donor, the UMFC continuously generated electricity with a maximum power density of 170 mW/m^2. To achieve this power density, the artificial electron-mediator hexacyanoferrate was required in the cathode chamber. The power density increased with increasing chemical oxygen demand (COD) loading rates up to 2.0 g COD/L/day after which no further increases in power density were observed, indicating the presence of limiting factors. The overarching limiting factor for the UMFC in this study was the internal resistance, which was estimated as 84 Ω at the maximum power density, and restricted the power output by causing a significant decrease in operating potential. Low Coulombic efficiencies varying from 0.7 to 8.1% implied that the electron-transfer bacteria were incapable of converting all of the available organics into electricity, so the excessive substrate created niches for the growth of methanogens. We found that the soluble COD (SCOD) removal efficiencies remained over 90% throughout the operational period, mainly because of methanogenic activity, which accounted for 35 to 58% of the SCOD removed at a loading rate of 1.0 g COD/L/day. Additionally, transport limitation due to insufficient substrate diffusion was shown by cyclic voltammetry (CV).

Introduction

The production of energy from wastewater is a high priority for our society given the current trends of population growth and worldwide energy resource depletion. Wastewater containing a high content of organic matter is an ideal commodity to produce alternative energy carriers, such as methane, hydrogen, and bioelectricity (*1*). In our electricity-based economy, bioelectricity is a promising alternative energy product generated from waste, because conversions from, for example, methane to a useful energy carrier (i.e., electricity) are not required. A bioelectricity generating wastewater treatment system at a single large food processing plant may power 900 American single-family households (*2*). Bioelectricity generation from wastewater is accomplished with microbial fuel cells (MFCs). In the anode chamber of a MFC, a microbial community oxidizes organic compounds from wastewater and transfers electrons to an electrode. Electrons flow from the anode to the cathode electrode through a conductive wire to generate current, while the produced protons diffuse through a proton-exchange membrane (PEM). Electrons and protons then react with oxygen molecules in the cathode chamber to form water. For most microbes, electron transfer to electrodes is not efficient due to electrically nonconductive cell walls and the obstruction from the peptide chain adjoining the active redox center of proteins (*3*). Such inefficiency is circumvented in MFCs by either adding artificial electron mediators or selecting for specific bacterial strains that can produce electron mediators or bacterial strains that have a strong ability to transfer electrons directly (*3*−*6*).

Over the past two decades researchers have been able to considerably increase power densities and Coulombic efficiencies to a maximum of 4,310 mW/m^2 and 89%, respectively (*2*, *7*−*9*). This maximum power density and high Coulombic efficiency was reached in a dual-chamber MFC with a well-acclimated, mixed-culture biofilm in the anode chamber and artificial soluble electron mediators in the cathode chamber while using plain graphite electrodes. High power densities and coulumbic efficiencies were achieved, however, at low volumetric loading rates (*8*, *9*). Low volumetric loading rates require reactors too large to be practical. Scale-up, will only be economical if volumetric loading rates can be increased without a decrease in Coulombic efficiency.

Power output is controlled by a number of factors, including the efficiency of electron transfer from microorganisms to electrodes, electrode surface area, the resistance of the electrolyte (i.e., anode and cathode solutions, and PEM), and the oxygen reaction kinetics in the cathode chamber. All of these factors can be grouped into three major categories (*10*): i. kinetic limitation, which occurs when energy is consumed to proceed reactions in anode and cathode chambers; ii. ohmic limitation, which is caused by the ionic resistance of electrolytes and the electric resistance of the electrodes and connection materials; and iii. transport limitation, which is due to the inefficient mass transport of substrates to the reaction sites within the bacterial cell. So far, only a few studies with MFCs have investigated the limiting factors. Oh et al. (*11*), for instance, found that power generation was limited by the cathode electrode surface area and that either adding an artificial electron mediator or increasing dissolved oxygen to the cathode chamber improved power output, which are ohmic and transport limitations, respectively. Based on electrochemical analysis Rabaey et al. (*9*), however, concluded that the electron transfer was affected by the production of extracellular electron mediator and the components related to the bacterial cell wall (i.e., kinetic limitations). Those studies have shown that the limiting factors must be identified and understood to improve the performance of MFCs.

Besides improving the power density by maintaining similar Coulombic efficiencies at higher volumetric loading rates, MFCs need to be converted to practical and economical wastewater treatment processes. The MFC with the highest power density of 4,310 mW/m^2 was fed as a batch-fed process and generated an irregular power output (*9*). Batch feeding is impractical for large-scale wastewater treatment process due to the need for a wastewater-holding tank. In addition, periodic feeding of wastewater cannot continuously mix the reactor, and supplementary mechanical mixing is required for batch-fed MFCs (*12*). The development of upflow anaerobic sludge blanket (UASB) reactors in the 1970s

* Corresponding author phone: (314) 935-5663; fax: (314) 935-5464; e-mail: angenent@seas.wustl.edu.
[†] Washington University in St. Louis.
[‡] Saint Louis University.

10.1021/es0502876 CCC: $30.25

Published on Web 06/09/2005

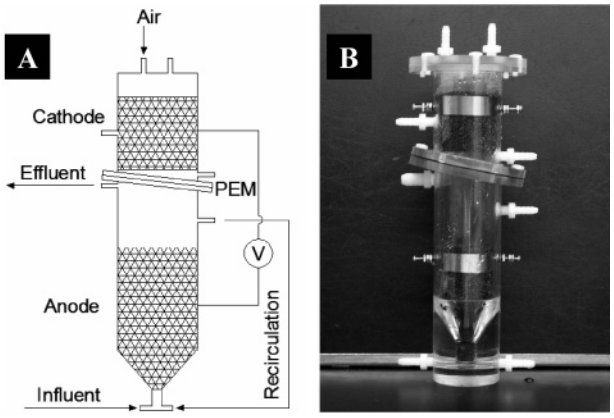

FIGURE 1. Schematic (A) and picture (B) of the lab-scale UMFC.

circumvented mechanical mixing for anaerobic digester bioreactors (*13*). Well-settling microbial aggregates appeared in the UASB due to a continuous selection pressure, which resulted in long biomass retention times and high biomass levels. These conditions accomplished the high-rate treatment of wastewater, which has made the UASB reactor financially competitive due to their relatively small reactor volumes.

We have developed a continuously fed MFC configuration, the upflow microbial fuel cell (UMFC), by combining the advantages of the UASB system with the requirements for a dual-chamber MFC. In addition, placing commercially available reticulated vitreous carbon (RVC) with a surface area of 51 m^2/m^3 ensures a large anode electrode surface even during the enlargement of the reactor volume during scale-up. This investigation monitored the power output of the UMFC during a natural selection process of an anodophilic biofilm (i.e., a biofilm that can efficiently transfer electrons to an electrode). The influence of limiting factors on the power output was also examined. Finally, the organic removal efficiency of the sucrose substrate was compared to a similarly operated UASB reactor.

Materials and Methods

UMFC. The UMFC comprised two cylindrical Plexiglas chambers with a 6-cm diameter. The cathode chamber (9-cm height, 250 cm^3 wet volume) was located on the top of the anode chamber (20-cm height, 520 cm^3 wet volume) (Figure 1). The anode and cathode chamber contained RVC (10 and 20 pores per inch (PPI), respectively, ERG, Oakland, CA) as electrodes, with a larger pore size porosity for the anode electrode to prevent biofilm clogging. The anode electrode (51 m^2/m^3) had a total volume of 190 cm^3 and surface area of 97 cm^2, while the cathode electrode (114 m^2/m^3) was 170 cm^3 in volume and 194 cm^2 in surface area. PEM (CMI-7000, Membrane International Inc., Glen Rock, NJ) was installed between two chambers with a 15° angle to the horizontal plane, which prevented accumulation of gas bubbles. Two side ports on the cathode chamber were used to replace the electron mediator weekly. The electrodes were connected by stainless steel in the chamber and copper wires externally to form a circuit.

UASB. The configuration of the UASB reactor was similar to Vallero et al. (*14*) and it was manufactured with a 6-cm diameter cylindrical Plexiglas. The working volume of the UASB was 650 cm^3, including a gas−solid separator phase of 200 cm^3. A reversed funnel used for gas collection had an angle of 75° over the horizontal plane. Glass beads with a 1-cm diameter were used to fill the bottom cone to promote fluid distribution.

Operating Conditions. The bioreactors were operated at 35 °C and continuously fed at a flow rate of 0.37 mL/min with sucrose solution at a 1.0-day hydraulic retention time (HRT) and a loading rate of 0.3−3.4 g COD/L/day. The artificial wastewater consisted of (per liter of deionized water): sucrose, 0.25−1.0 g; NH_4Cl, 0.2 g; $CaCl_2{\cdot}2H_2O$, 0.15 g; KCl, 0.33 g; NaCl, 0.30 g; $MgCl_2$, 3.15 g; K_2HPO4, 1.26 g; KH_2PO_4, 0.42 g; trace metals (1 mL) (*15*) and yeast extract (0.25−1.0 g). The sucrose solution was maintained at 4 °C. Effluent of the anode chamber was recirculated at a flow rate of 45 mL/min and mixed with influent to maintain an upflow velocity in the anode chamber of 1 m/h. Granular anaerobic sludge from a mesophilic upflow anaerobic bioreactor treating brewery wastewater was used to inoculate the UMFC and UASB reactors. Before inoculation, the sludge was ground with a mortar and pestle, and then filtered through a 0.25-mm pore size sieve to remove large particles. The cathode chamber was filled with 100 mM potassium hexacyanoferrate (Sigma-Aldrich, St.Louis, MO) as an artificial electron mediator.

Chemical Analysis. The concentrations of chemical oxygen demand (COD) in influent and soluble COD (SCOD) and volatile fatty acids (VFAs) in effluent were determined according to procedures described in *Standard Methods* (*16*). The concentration of VFA was expressed as mg acetic acid per liter. Biogas production was measured by a wet gas meter (Actaris Meterfabriek BV, Delft, The Netherlands). The composition of biogas was analyzed using a gas chromatograph (Series 350, GOW-MAC, Bethlehem, PA) with a thermal conductivity detector. The temperatures of the injection port and detector were 20 and 40 °C, respectively. Helium was used as the carrier gas at a flow rate of 60 mL/min.

Electrochemical Measurement. The voltage (V) across a resistor (R) was measured by a data acquisition module (OMR6017, Omega Engineering Inc., Stamford, CT). Data were recorded to a personal computer every 30 s. Current (I) was determined by Ohm's law ($I = V/R$), and power density of the UMFC was calculated as $P = VI/A$, where A was the surface area of anode electrode. The internal resistance (R_i) was estimated as V_d/I, where V_d was the difference between open circuit potential and the voltage across the external resistor. Coulombic efficiency was described as the ratio of the output charge (Q_{out}) to the input charge (Q_{in}). The output charge was calculated by integrating the current over time as $Q_{out} = \sum (It)$, where t is the time. The input charge was expressed as (*8*):

$$Q_{in} = 96485(\mathrm{C/mol\ e^-}) \times \frac{COD_i(\mathrm{g\ O_2/mL}) \times W \times t \times 60}{32(\mathrm{g\ O_2/mol\ O_2})} \times 4(\mathrm{mol\ e^-/mol\ O_2}) \quad (1)$$

where W is the flow rate (mL/min) and COD_i is the influent COD. Energy recovery was calculated according to Liu et al. (*17*), and the enthalpy change was based on the following reaction:

$$C_{12}H_{22}O_{11} + 12O_2 = 12CO_2 + 11H_2O \quad (2)$$

A polarization curve was generated by varying the resistance from 10 to 1470Ω. Data from each resistor was recorded after a stable voltage was achieved with a minimum connection time period of 3 h.

Cyclic Voltammetry (CV). In this study, CV was performed with a potentiostat (601B, CH Instruments, Austin, TX) interfaced to a personal computer. A glassy carbon working electrode (3.0 mm in diameter), an Ag/AgCl reference electrode, and a platinum counter electrode (all from CH Instruments) were used in a 15-ml electrochemical cell. Before and after each measurement, the working electrode was polished with alumina powder (0.05 microns, CH Instruments). Fifteen milliliter of biofilm sample was removed

from the UMFC. This was immediately centrifuged at 9300 × g and the pellets were resuspended in 10-ml sucrose solution in the electrochemical cell. Nitrogen gas was used to continuously flush the electrochemical cell throughout the experiment. Data were recorded after a one-day acclimation period to grow biofilm on the working electrode. Four scan rates of 10, 30, 50 and 70 mV/s were employed with 15 min of equilibration between scans. The CV experiment scanned the potential range from −0.7 to 0.7 V vs Ag/AgCl. Several cycles were performed in sequence and the peak current (i_P) vs the square root of scan rate ($v^{1/2}$) was plotted for each cycle. The linearity of the plot from each cycle was used to analyze the limiting factors (transport vs kinetic).

Cyclic voltammograms contain a forward and reverse scan, which generate a positive wave and a negative wave corresponding to reduction and oxidation in this study. The positive wave is usually used for analysis, because positive and negative waves will theoretically generate identical peak currents, while the negative peak is harder to measure due to background electrolysis. The relationship between the peak current and the scan rate can be used to study kinetic and transport limitations in the system. According to Bard and Faulkner (*18*), when transport limitation (diffusion) dominates in the system, the peak current is proportional to the square root of the scan rate:

$$i_p = (2.99 \times 10^5)\alpha^{1/2} A C_0 D_0^{1/2} v^{1/2} \quad (3)$$

where α is the transfer coefficient for the reaction; A is the surface area of the anode electrode (cm^2); C_0 is the initial concentration of substrate in the bulk solution (mol/cm^3); D_0 is the diffusion coefficient of the substrate (cm^2/s); and v is the scan rate (V/s).

Fluorescence In Situ Hybridization (FISH). The biomass attached to the anode electrode was removed and fixed with 4% paraformaldehyde for 2 h at 4 °C and stored with phosphate buffer saline solution and ice-cold ethanol at −20 °C. Hybridization was performed with 16S rRNA-targeting oligonucleotide DNA probes specific for Archaea (ARC 915) (*19*) and Bacteria (EUB 338) (*20*) according to de los Reyes et al. (*21*). Specimens were viewed with an epifluorescence microscope (BX41, Olympus, Melville, NY) and digital images were taken with a CCD camera (QImaging, Burnaby, Canada.) and saved in Openlab 3.5 software (Improvision Inc., Lexington, MA). Images were overlaid in Photoshop 7 (Adobe System, Seattle, WA).

Results and Discussion

UMFC Electricity Generation. The UMFC was fed with a sucrose solution continuously for five months, generating electricity over the entire operating period and achieving a constant SCOD removal. The UMFC is operated in a continuous mode, which is more practical for further scale-up than the batch-fed operation adopted by most researchers. The UMFC was fed at a loading rate of 1.0 g COD/L/day and a flow rate of 0.36 mL/min during the start of operation. The open circuit potential reached 0.75 V on day 3 of the operational period, and current was produced after an external resistor was connected. To examine the dependence of current production on substrate oxidation, the sucrose solution was replaced by tap water on day 20. The current decreased to half of the original value within 2 days, and was only restored when sucrose solution was resumed, indicating that substrate oxidation was essential for electricity generation. The characteristics of UMFC electricity generation were examined by a polarization curve, which showed that the maximum power density of 170 mW/m^2 occurred at 66 Ω (0.33V) with a current density of 516 mA/m^2 (days 25−37; Figure 2). Calculated by eq 1, the Coulombic efficiency at this power density was 8.1%. Figure 2 also showed that open circuit potential and short circuit current density were 0.74 V and 960 mA/m^2, respectively.

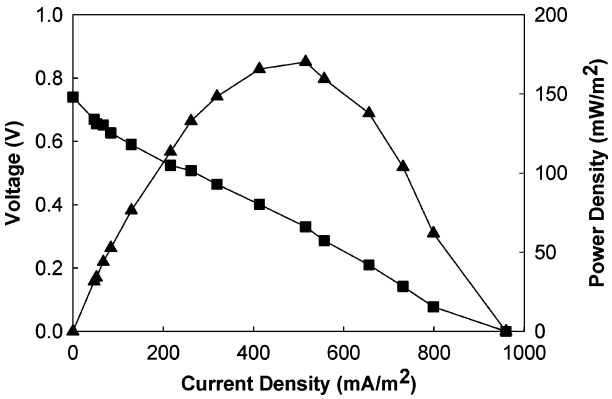

FIGURE 2. Polarization curve for UMFC at a 1-day HRT and a COD loading rate of 1.0 g COD/L/day. Voltage (■) and power density (▲). This test was performed between days 25−37. The maximum power density was 170 mW/m^2 at a current density of 516 mA/m^2.

Internal Resistance (R_i). The maximum power density of the UMFC was lower than that of some previous studies with MFCs (*9*, *17*, *22*). The most likely explanation for a lower output was a relatively large R_i, which restricted the power output by causing a significant decrease in operating potential due to ohmic limitations. The R_i of the UMFC was around 84 Ω at a power density of 170 mW/m^2, by a rough estimation according to equation ($R_i = V_d/I$). A similar estimation with the information from Rabaey et al. (*9*), showed an R_i of 3 Ω for their dual-chamber MFC, 20 times smaller than the R_i of the UMFC, and therefore a higher current of 30.9 mA was achieved (the maximum current for our UMFC was 9.31 mA). Since generally the electromotive force (open circuit potential) is ∼0.75 V, the UMFC would not be able to generate a power density higher than 720 mW/m^2 (i.e., 0.75V × 9.31mA/97 cm^2). Thus, the R_i must be reduced to improve the power output of the UMFC, especially as a slight reduction in R_i can dramatically improve a fuel cell's power density (*23*). The most likely cause of the R_i for the UMFC was the large resistance to transfer of protons through the electrolyte solutions, due to the significant distance between anode and cathode electrodes. Transfer resistance of protons through the PEM and resistance due to slow reduction reactions on the cathode electrode are unlikely, because we used a similar PEM and cathode electron-mediators materials as Rabaey et al. (*9*). The electric resistances of carbon electrodes and RVC electrodes were similar (*24*). Therefore, the 84-Ω R_i of the UMFC appeared to be due to reactor configuration problems rather than reactor materials.

The high proton-transfer resistance was observed in the UMFC, because the protons were not moving fast enough at a high current to meet the proton production on the anode (*25*). This was consistent with the pH reduction from 6.65 to 5.11, which was observed in the anode chamber at the high current of 3.9 mA and a low external resistance of 100 Ω (day 40−46). A similar pH drop from 6.66 to 5.28 was found during day 60−65 when this experiment was repeated. In addition to the pH drop, the VFA concentration increased from 127 to 280 mg/L during days 40−46, ultimately resulting in a decreased power output as reflected by a sudden current drop from 3.2 to 2.2 mA on day 45 (Figure 3). During the same period, the pH of the cathode solution remained constant (data not shown). This phenomenon was not observed at higher external resistances of 250 and 470 Ω and a resulting lower current, which indicated both a lower demand for protons on the cathode reaction and sufficient proton transfer in the UMFC. Results also implied that the

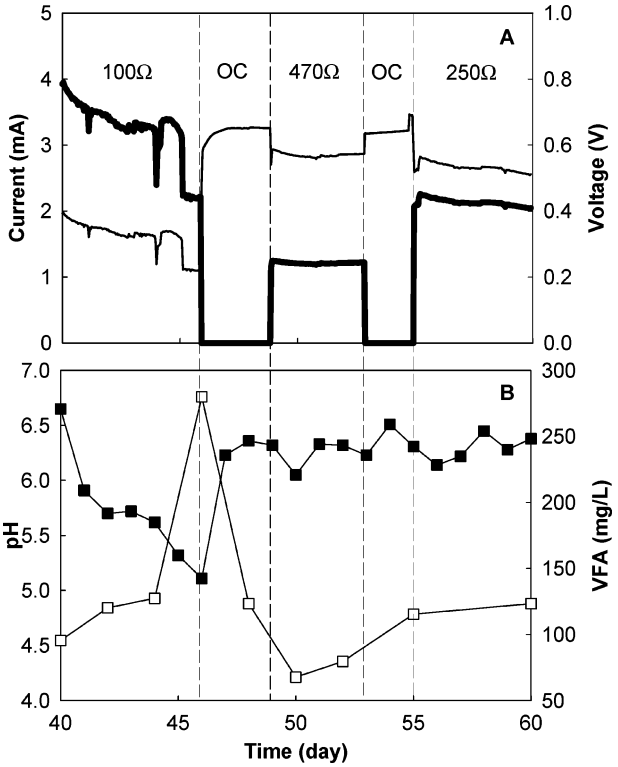

FIGURE 3. Effect of current on proton transfer: (A) variation of current (bold line) and voltage (thin line) at different external resistances; (B) variation of the pH in the anode chamber (■) and VFA concentration in effluent (□). The loading rate was 1.0 g COD/L/day during this period. OC indicates open circuit when the current was zero.

pH in the bioreactor may be controlled by changing the external resistance, which could be used to optimize the environmental condition in anode chamber.

UMFC Methane Formation. The presence of a large R_i, as well as other limiting factors, restricted the capacity of the UMFC to generate power, and therefore the rate of electron transfer by bacteria to the electrode. The low Coulombic efficiencies indicated that organic loading was beyond the oxidation abilities of the anodophilic bacteria, and that the substrate was oxidized by other anaerobic microbes, such as nitrate-reducing bacteria, sulfate-reducing bacteria, or methanogenic archaea. Methanogens grow and produce methane in an environment with a reducing potential less than −330 mV (*26*). In a MFC, the anode potential is normally higher than 0 mV compared to a standard hydrogen electrode (*9*). Such a potential is very unfavorable for the growth of methanogens, and therefore no methane formation was observed during start up in a dual-chamber MFC with consistently high Coulombic efficiencies (*8*). However, during the operation of the UMFC, we found a significant amount of methane production, because an excess of substrate provided an unforeseen niche for methanogens. This finding was consistent with a recent study that reported methane production in a dual-chamber MFC (*27*). At a loading rate of 1.0 g COD/L/day, the methane yield for the UMFC varied between 130 and 220 mL/g SCOD removed, which accounted for 35 and 58% of SCOD removed, respectively. FISH images clearly showed archaea (i.e., methanogens) in the mixed biomass community sampled from the surface of the anode electrode (Figure 4).

To study the substrate-niche hypothesis and to test if methanogens were not simply out competing electron-transferring bacteria for substrate, we selectively inhibited the growth of methanogens by adding 6 mM 2-bromoethanesulfonate (BES) to a dual-chamber MFC. No methane production was observed after addition of BES, and the power density increased by 25% (data not shown). If methanogens had been actively competing for substrate with the anodophilic bacteria, a larger increase in power density was expected. The results, thus, indicated that methanogens were able to grow only because excess substrate was available. This fact will have important consequences for MFCs treating wastewater, because methanogenesis must be anticipated whenever the substrate (i.e., electron) loading rate is greater than the maximum equivalent electron-transfer rate of the MFC under shock-load conditions. Periodic aeration may prevent methanogens from inhabiting electrode biofilms.

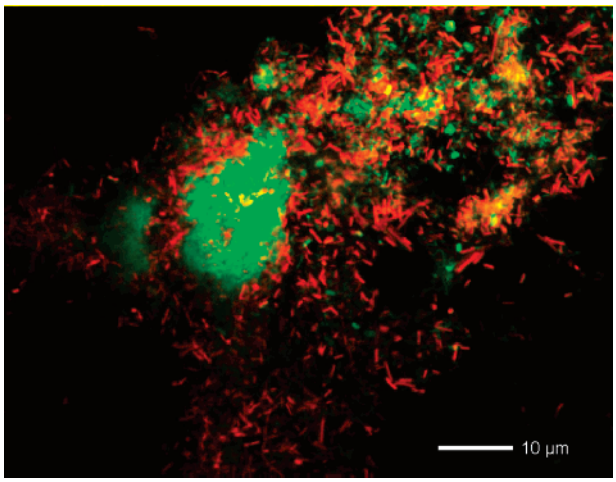

FIGURE 4. FISH image of the biomass sampled from the anode electrode on day 85. Archaeal- (ARC915, green) and bacterial-specific oligonucleotide probes were used (EUB338, red).

SCOD Removal. Since methanogens consumed the extra organics that electron-transfer bacteria could not decompose, the UMFC achieved a high SCOD removal efficiency. The influence of COD loading rates on power output and SCOD removal efficiencies was examined from day 90. First, the open circuit potential was decreased below 0.2 V by feeding tap water to reduce the interference of remaining substrates from the previous operation. Next, the COD loading rates were varied from 0.3 to 3.4 g COD/L/day at a constant hydraulic retention time of 1.0 day and a 300-Ω external resistor. Increases in loading rate were made only after a stable SCOD removal efficiency was achieved. The results showed that the highest power density of 92.9 mW/m^2 occurred at a loading rate of 2.0 g COD/L/day and did not noticeably change with increasing loading rates; while the Coulombic efficiency decreased from 7.1 to 0.7% (Figure 5A) and the overall energy recovery based on electricity from sucrose decreased from 6.1 to 0.7% with increasing loading rates. The SCOD removal efficiency increased at a higher COD loading rate in which the highest SCOD removal efficiency (97%) was obtained at the highest loading rate of 3.4 g COD/L/day (Figure 5B). The low Coulombic efficiency and the high SCOD removal efficiency indicated that the majority of SCOD was removed by methanogens or other microbes, instead of the electron-transfer bacteria.

During the parallel operation of UMFC and UASB, we found that both reactors achieved statistically insignificant difference in SCOD and VFA concentrations in effluent (data not shown). Generally, SCOD removal efficiencies were greater than 90% and effluent VFA concentrations were usually lower than 100 mg/L. A similar UMFC performance compared to the UASB reactor implied that our UMFC configuration was suitable to efficiently remove organic material from wastewater.

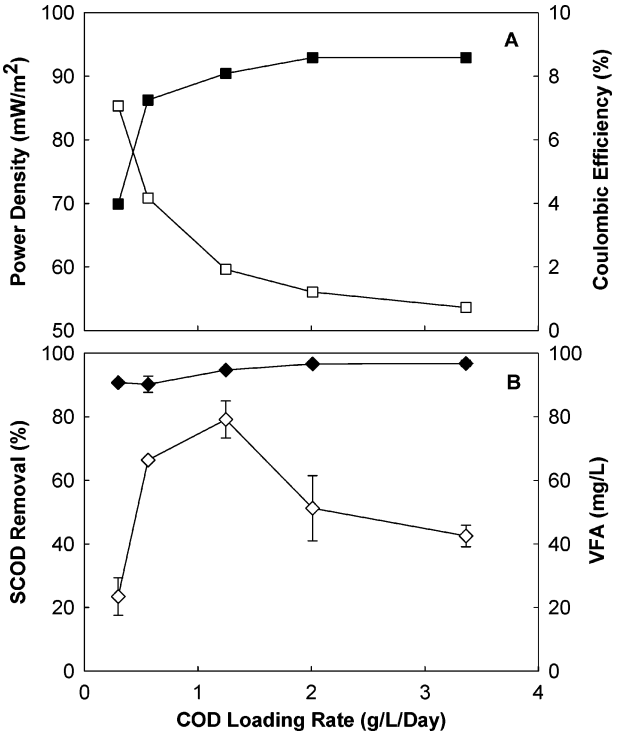

FIGURE 5. Influence of COD loading rates on (A) power density (■) and Coulombic efficiency (□), and (B) SCOD removal efficiency (◆) and VFA concentration (◇) (300 Ω, 1-day HRT) during the operation period between day 90 and 130. Values of SCOD removal and VFA concentration were the mean of duplicate measurements. Bars represent standard errors.

Transport Limitation. Besides ohmic limitations, we also studied kinetic and transport limitations for the anode biofilm in a separate electrochemical cell using CV (biofilm samples were taken from the UMFC and UASB reactors on day 85). By plotting the peak current vs the square root of scan rates in one cycle (four scan rates in sequence), a straight line was obtained with a R^2 of 0.9980 ± 0.0018 for 10 cycles. According to eq 3, the linear relationship between peak currents and the square root of scan rates indicated that transport (diffusion) limitation would have a greater contribution to potential losses than kinetic limitation in the anode biofilm if the R_i had been low in the UMFC. At an 84-Ω R_i we anticipate the transport limitation to play only a minor role, but this may become more prominent during further development of the UMFC in which we will reduce the R_i. In addition, reduction/oxidation peaks were observed for the anode biofilm (line a, Figure 6), which shows electrochemical activity. Biomass from the UASB reactor, taken at the same time, did not show a significant electrochemical activity (line b, Figure 6) and generated a similar current shape as that of a biomass-free electrode (line c, Figure 6). UMFC and UASB reactors were inoculated with similar anaerobic granular biomass, and thus exclusive electrochemical activity in the anode biofilm of the UMFC shows selection and enrichment for anodophilic bacteria.

Outlook for Full Scale Operation. The primary goal of wastewater treatment is to remove organic pollutants. The UMFC has achieved this goal by removing over 90% SCOD from the sucrose solution. If a UMFC with a working volume of 7,500 m^3 contains a 51 m^2/m^3 anode electrode, at a maximum power output of 170 mW/m^2, we can generate 1530 kWh/day of electricity (24-hour operation) or 0.204 kWh/m^3 water treated. This is close to 0.25 kWh/m^3 consumed by an aerobic trickling filter (*28*), which implies that UMFC bioreactors can potentially provide enough electricity for its own operation. However, we must realize that, after overcoming high R_i limitation in UMFC, electricity generation from a real wastewater will be lower than from an artificial wastewater, which was used in this study. We also calculated the electric energy production of an existing UASB reactor with a similar volume of 7,500 m^3. For the UASB electricity calculation we adopted a typical loading rate of 15 g COD/L/day, a 65% total COD removal efficiency, and a methane-to-electricity conversion efficiency of 30%, and obtained a daily electricity generation of 75,779 kWh/day. This is 49 times higher than that for the UMFC. To develop a system that can out compete existing UASB systems in regards to electricity production, the power density of UMFCs must be improved to 8,500 mW/m^2. This is within reach by first elucidating the mechanisms of limiting factors followed by modifying UMFC configuration and operation.

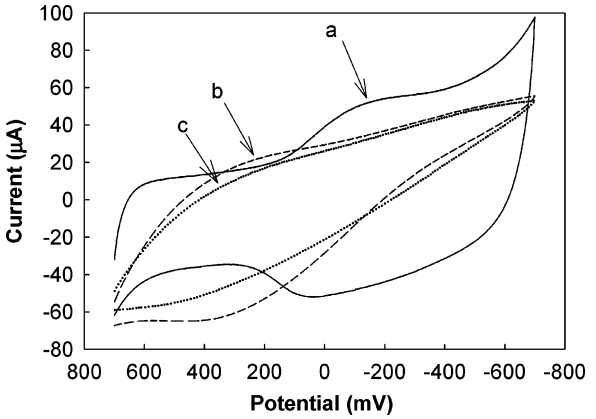

FIGURE 6. Cyclic voltammograms of biomass grown in UMFC (solid line a) and UASB (dashed line b), and a biomass-free electrode (dotted line c). Scan rate was 0.05 mV/s. Biofilm samples were taken on day 85.

Acknowledgments

We thank Jack Loren (Membranes International Inc.) for donating PEM, Joe Doll (ERG Materials and Aerospace Corporation) for donating RVC, Becky Treu (Saint Louis University) for assistance with CV, and Brian Wrenn (Washington University in St. Louis), members of the Angenent Lab and anonymous reviewers for helpful comments. Support for this work was provided by the Jen's endowment.

Literature Cited

(1) Angenent, L. T.; Karim, K.; Al-Dahhan, M. H.; Wrenn, B. A.; Domiguez-Espinosa, R. Production of bioenergy and biochemicals from industrial and agricultural wastewater. *Trends Biotechnol.* **2004**, *22*, 477−485.

(2) Logan, B. E. Feature Article: Biologically extracting energy from wastewater: biohydrogen production and microbial fuel cells. *Environ. Sci. Technol.* **2004**, *38*, 160A-167A.

(3) Kim, H. J.; Park, H. S.; Hyun, M. S.; Chang, I. S.; Kim, M.; Kim, B. H. A mediator-less microbial fuel cell using a metal reducing bacterium, *Shewanella putrefaciens*. *Enzyme Microb. Technol.* **2002**, *30*, 145−152.

(4) Park, D. H.; Zeikus, J. G. Electricity generation in microbial fuel cells using neutral red as an electronophore. *Appl. Environ. Microbiol.* **2000**, *66*, 1292−1297.

(5) Pizzariello, A.; Stred'ansky, M.; Miertus, S. A glucose/hydrogen peroxide biofuel cell that uses oxidase and peroxidase as catalysts by composite bulk-modified bioelectrodes based on a solid binding matrix. *Bioelectrochemistry* **2002**, *56*, 99−105.

(6) Chaudhuri, S. K.; Lovley, D. R. Electricity generation by direct oxidation of glucose in mediatorless microbial fuel cells. *Nat. Biotechnol.* **2003**, *21*, 1229−1232.

(7) Bennetto, H. P. Electricity generation by microorganisms. *Biotechnology Education* **1990**, *1*, 163−168.

(8) Rabaey, K.; Lissens, G.; Siciliano, S. D.; Verstraete, W. A microbial fuel cell capable of converting glucose to electricity at high rate and efficiency. *Biotechnol. Lett.* **2003**, *25*, 1531−1535.

(9) Rabaey, K.; Boon, N.; Siciliano, S. D.; Verhaege, M.; Verstraete, W. Biofuel cells select for microbial consortia that self-mediate electron transfer. *Appl. Environ. Microbiol.* **2004**, *70*, 5373−5382.
(10) Appleby, A. J.; Foulkes, F. R. *Fuel Cell Handbook*; Van Nostrand Reinhold: New York, 1989.
(11) Oh, S. E.; Min, B.; Logan, B. E. Cathode performance as a factor in electricity generation in microbial fuel cells. *Environ. Sci. Technol.* **2004**, *38*, 4900−4904.
(12) Bond, D. R.; Lovley, D. R. Electricity production by *Geobacter sulfurreducens* attached to electrodes. *Appl. Environ. Microbiol.* **2003**, *69*, 1548−1555.
(13) Lettinga, G.; van Velsen, A. F. M.; Hobma, S. W.; de Zeeuw, W.; Klapwijk, A. Use of the upflow sludge blanket (USB) reactor concept for biological wastewater treatment, especially for anaerobic treatment. *Biotechnol. Bioeng.* **1980**, *22*, 699−734.
(14) Vallero, M. V. G.; Trevino, R. H. M.; Paulo, P. L.; Lettinga, G.; Lens, P. N. L. Effect of sulfate on methanol degradation in thermophilic (55C) methanogenic UASB reactors. *Enzyme Microb. Technol.* **2003**, *32*, 676−687.
(15) Angenent, L. T.; Sung, S. Development of anaerobic migrating blanket reactor (AMBR), a novel anaerobic treatment system. *Water Res.* **2001**, *35*, 1739−1747.
(16) Clesceri, L. S.; Greenberg, A. E.; Eaton, A. D. *Standard Methods for the Examination of Water and Wastewater*; 20th ed.; American Public Health Association: Washington, DC, 1998.
(17) Liu, H.; Cheng, S.; Logan, B. E. Production of electricity from acetate or butyrate using a single-chamber microbial fuel cell. *Environ. Sci. Technol.* **2005**, *39*, 658−662.
(18) Bard, A. J.; Faulkner, L. R. *Electrochemical Methods-Fundamentals and Applications*; 2nd ed.; John Wiley & Sons: 2001.
(19) Stahl, D. A.; Amann, R. I. In *Nucleic Acids Techniques in Bacterial Systematics*; Stackebrandt, E., Goodfellow, M., Eds.; John Wiley & Sons: New York, 1991; pp 205−248.
(20) Amann, R. I.; Krumholz, L.; Stahl, D. A. Fluorescent-oligonucleotide probing of whole cells for determinative, phylogenetic, and environmental studies in microbiology. *J. Bacteriol* **1990**, *172*, 762−770.
(21) de los Reyes, F. L.; de los Ritter, W.; Raskin, L. Group-specific small subunit rRNA hybridization probes to characterize filamentous foaming in activated sludge system. *Appl. Environ. Microbiol.* **1997**, *63*, 1107−1117.
(22) Park, D. H.; Zeikus, J. G. Improved fuel cell and electrode designs for producing electricity from microbial degradation. *Biotechnol. Bioeng.* **2003**, *81*, 348−355.
(23) Mench, M. M.; Wang, C.; Thynell, S. T. An introduction to fuel cell and related transport phenomena. *I. J. Trans. Phenomena* **2001**, *3*.
(24) Wang, J. Reticulated vitreous carbon − a new versatile electrode material. *Electrochim. Acta* **1981**, *26*, 1721−1726.
(25) Gil, G. C.; Chang, I. S.; Kim, B. H.; Kim, M.; Jang, J. K.; Park, H. S.; Kim, H. J. Operational parameters affecting the performannce of a mediator-less microbial fuel cell. *Biosens. Bioelectron.* **2003**, *18*, 327−334.
(26) Lange, M.; Ahring, B. K. A comprehensive study into the molecular methodology and molecular biology of methanogenic Archaea. *FEMS Microbiol. Rev.* **2001**, *25*, 553−571.
(27) Kim, J. R.; Min, B.; Logan, B. E. Evaluation of procedures to acclimate a microbial fuel cell for electricity production. *Appl. Microbiol. Biotechnol.* **2005**, In press.
(28) Burton, F. L. "Water and wastewater industries: characteristics and energy management opportunities," Burton Environmental Engineering, 1996.

Received for review February 11, 2005. Revised manuscript received April 27, 2005. Accepted April 29, 2005.

ES0502876